# $a_0^+(980)$-resonance production in the reaction $pp \to d\pi^+\eta$ close to the $K\bar{K}$ threshold

P. Fedorets,[1,2] M. Büscher,[1] V.P. Chernyshev,[2] S. Dymov,[1,3] V.Yu. Grishina,[4] C. Hanhart,[1] M. Hartmann,[1] V. Hejny,[1] V. Kleber,[5] H.R. Koch,[1] L.A. Kondratyuk,[2] V. Koptev,[6] A.E. Kudryavtsev,[2] P. Kulessa,[1] S. Merzliakov,[3] S. Mikirtychiants,[6] M. Nekipelov,[1,6] H. Ohm,[1] R. Schleichert,[1] H. Ströher,[1] V.E. Tarasov,[2] K.-H. Watzlawik,[1] and I. Zychor[7]

[1] *Institut für Kernphysik, Forschungszentrum Jülich, 52425 Jülich, Germany*
[2] *Institute for Theoretical and Experimental Physics, Bolshaya Cheremushkinskaya 25, 117218 Moscow, Russia*
[3] *Laboratory of Nuclear Problems, Joint Institute for Nuclear Research, 141980 Dubna, Russia*
[4] *Institute for Nuclear Research, 60th October Anniversary Prospect 7A, 117312 Moscow, Russia*
[5] *Institut für Kernphysik, Universität zu Köln, Zülpicher Str. 77, 50937 Köln, Germany*
[6] *High Energy Physics Department, Petersburg Nuclear Physics Institute, 188350 Gatchina, Russia*
[7] *The Andrzej Soltan Institute for Nuclear Studies, 05400 Swierk, Poland*



The reaction $pp \to d\pi^+\eta$ has been measured at a beam energy of $T_p$=2.65 GeV ($p_p$=3.46 GeV/c) using the ANKE spectrometer at COSY-Jülich. The missing mass distribution of the detected $d\pi^+$ pairs exhibits a peak around the $\eta$ mass on top of a strong background of multi-pion $pp \to d\pi^+(n\pi)$ events. The differential cross section $\mathrm{d}^4\sigma/\mathrm{d}\Omega_d\mathrm{d}\Omega_{\pi^+}\mathrm{d}p_d\mathrm{d}p_{\pi^+}$ for the reaction $pp \to d\pi^+\eta$ has been determined model independently for two regions of phase space. Employing a dynamical model for the $a_0^+$ production allows one then to deduce a total cross section of $\sigma(pp \to da_0^+ \to d\pi^+\eta) = (1.1 \pm 0.3_{\mathrm{stat}} \pm 0.7_{\mathrm{sys}})$ $\mu$b for the production of $\pi^+\eta$ via the scalar $a_0^+(980)$ resonance and $\sigma(pp \to d\pi^+\eta) = (3.5 \pm 0.3_{\mathrm{stat}} \pm 1.0_{\mathrm{sys}})$ $\mu$b for the non-resonant production. Using the same model as for the interpretation of recent results from ANKE for the reaction $pp \to dK^+\bar{K}^0$, the ratio of the total cross sections is $\sigma(pp \to d(K^+\bar{K}^0)_{L=0})/\sigma(pp \to da_0^+ \to d\pi^+\eta) = 0.029 \pm 0.008_{\mathrm{stat}} \pm 0.009_{\mathrm{sys}}$, which is in agreement with branching ratios in the literature.

## I. INTRODUCTION

One of the primary goals of hadronic physics is the understanding of the internal structure of mesons and baryons, and their production and decay, in terms of quarks and gluons. The non-perturbative character of the underlying theory — Quantum Chromo Dynamics (QCD) — hinders straightforward calculations. QCD can be treated explicitly in the low momentum-transfer regime using lattice techniques [1], which are, however, not yet in the position to make quantitative statements about the light scalar mesons. Alternatively, QCD-inspired models, which employ effective degrees of freedom, can be used. The constituent quark model is one of the most successful in this respect (see e.g. [2]). This approach treats the lightest scalar resonances $a_0/f_0(980)$ as conventional $q\bar{q}$ states.

However, more states with quantum numbers $J^P$=$0^+$ have been identified experimentally than would fit into a single SU(3) scalar nonet: the $f_0(600)$ (or $\sigma$), $f_0(980)$, $f_0(1370)$, $f_0(1500)$ and $f_0(1710)$ with $I$=0, the $\kappa(800)$ and $K^*(1430)$ ($I$=1/2), as well as the $a_0(980)$ and $a_0(1450)$ ($I$=1) [3]. Consequently, the $a_0/f_0(980)$ have also been associated with $K\bar{K}$ molecules [4] or compact $qq$-$\bar{q}\bar{q}$ states [5]. It has even been suggested that a complete nonet of four-quark states might exist with masses below 1.0 GeV/c$^2$ [6].

The first clear observation of the isovector $a_0(980)$ resonance was achieved in $K^-p$ interactions [7], and in subsequent experiments it has also been seen in $p\bar{p}$ annihilations [8], in $\pi^-p$ collisions [9], and in $\gamma\gamma$ interactions [10]. Experiments on radiative $\phi$-decays [11, 12] have been analysed in terms of the $a_0/f_0$ production in the decay chain $\phi \to \gamma a_0/f_0 \to \gamma\pi^0\eta/\pi^0\pi^0$. In $pp$ collisions the $a_0(980)$ resonance has been measured at $p_p = 450$ GeV/c *via* $f_1(1285) \to a_0^\pm\pi^\mp$ decays [13] and in inclusive measurements of the $pp \to dX^+$ reaction at $p_p$ = 3.8, 4.5, and 6.3 GeV/c [14]. Despite these many experimental results, the properties of the $a_0(980)$ resonance are still far from being established. The Particle Data Group gives a mass of $m_{a_0} = (984.7 \pm 1.2)$ MeV/c$^2$ and a width of $\Gamma_{a_0} = (50 - 100)$ MeV/c$^2$ [3]. The main decay channels, $\pi\eta$ and $K\bar{K}$, are quoted as "dominant" and "seen" respectively.

An experimental programme has been started at the Cooler Synchrotron COSY-Jülich [15] aiming at exclusive data on the $a_0/f_0$ production from $pp$, $pn$, $pd$ and $dd$ interactions at energies close to the $K\bar{K}$ threshold [16]. The final goal of these investigations is the extraction of the $a_0/f_0$-mixing amplitude, a quantity which is believed to shed light on the nature of these resonances [17, 18]. As a first stage the reaction $pp \to dK^+\bar{K}^0$ has been measured at $T_p$=2.65 GeV, corresponding to an excess energy of $Q$=46 MeV above the $K^+\bar{K}^0$ threshold, using the ANKE spectrometer [19]. The data, which have been decomposed into partial waves, show that more that 80% of the kaons are produced in a relative $s$–wave, corresponding to the $a_0^+$ channel [20]. In this paper we report on the analysis of the reaction $pp \to d\pi^+\eta$, which was measured in parallel.

## II. THE ANKE SPECTROMETER AND DATA ANALYSIS

Fig. 1 shows the layout of ANKE. It consists of three dipole magnets (D1 – D3), installed at an internal tar-

get position of COSY. D1 and D3 deflect the circulating COSY beam from and back into the nominal orbit. The C-shaped spectrometer dipole D2 separates forward-going reaction products from the COSY beam. The angular acceptance of ANKE covers $|\vartheta_{\rm h}| \leq 10^\circ$ horizontally and $|\vartheta_{\rm v}| \leq 3^\circ$ vertically for the detected deuterons ($p_d > 1300$ MeV/c), and $|\vartheta_h| \leq 12^\circ$ and $|\vartheta_v| \leq 3.5^\circ$ for the pions. An $H_2$ cluster-jet target [21], placed between D1 and D2, has been used, providing areal densities of $\sim 5\times10^{14}\,{\rm cm}^{-2}$. The luminosity has been measured using $pp$ elastic scattering, recorded simultaneously with the $d\pi^+$ data. Protons in the angular range $\vartheta = 5.5^\circ - 9^\circ$ have been selected, since the ANKE acceptance changes smoothly in this region and the elastic peak is easily distinguished from the background in the momentum distribution. The average luminosity during the measurements has been determined as $L = (2.7\pm0.1_{\rm stat}\pm0.7_{\rm syst})\times10^{31}\,{\rm s}^{-1}\,{\rm cm}^{-2}$, corresponding to an integrated value of $L_{\rm int} = 3.3\,{\rm pb}^{-1}$ at a proton beam intensity of up to $\sim 4\times10^{10}$.

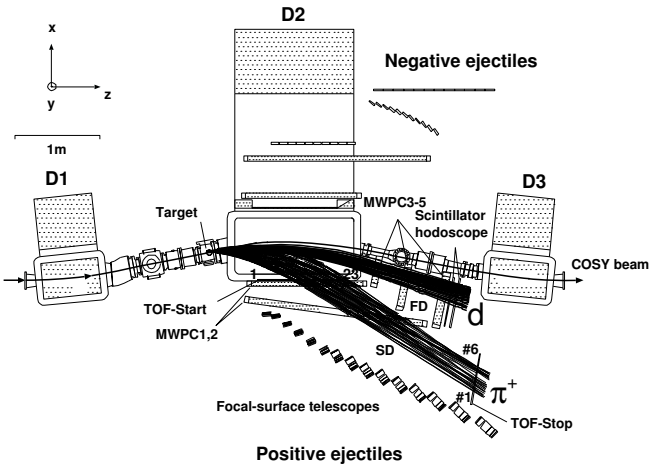


FIG. 1: Top view of the ANKE spectrometer and simulated tracks of pions and deuterons from $pp \to d\pi^+\eta$ events.

Two charged particles, $\pi^+$ and $d$, were detected in coincidence. Their trajectories, simulated with the ANKE-GEANT program package [22], are shown in Fig. 1. Positively charged pions in the momentum range $p_\pi = (600 - 1100)$ MeV/c were identified in the side detection system (SD) [19, 23], consisting of one layer of 23 start time-of-flight (TOF) scintillation counters, two multiwire proportional chambers (MWPCs) and one layer of 6 counters for TOF-stop. Pions were selected by a time-of-flight technique (Fig. 2a). The fast deuterons with momenta $p_d = (1300 - 2800)$ MeV/c (and elastically scattered protons with $p_p \approx 3400$ MeV/c) hit the forward detection system (FD) [19, 24], which includes three MWPCs and two layers of scintillation counters. Two-dimensional distributions $\Delta t$ *vs.* momenta of forward particles have been used for the deuteron identification. $\Delta t$ was calculated as the time difference between the detection of a pion in the TOF-stop counter and a fast forward-going particle in the first layer of the FD scintillators. Two distinct bands corresponding to protons and deuterons are seen in this distribution (Fig. 2b). The selection of deuterons was achieved by cutting along the deuteron band.

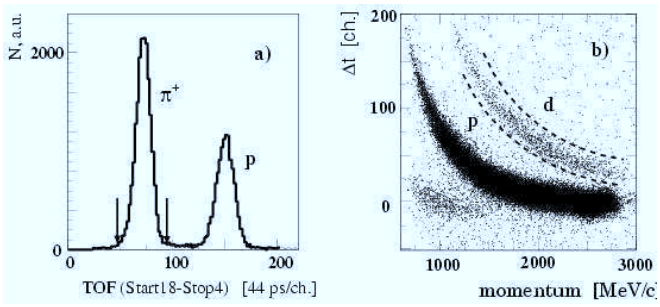


FIG. 2: a) Time-of-flight of particles detected in TOF start counter 18 and stop counter 4; b) time difference $\Delta t$ between fast forward-going particles in the FD and $\pi^+$ mesons as a function of the momentum of the forward particle. The dashed lines indicate the criteria for deuteron identification.

The tracking efficiency for pions in the SD MWPCs was calculated as the ratio of particles in the proper TOF range with and without requiring a reconstructed track. The efficiency depends on the SD stop-counter number (i.e. $\pi^+$ momentum) and varies between 53% and 76%. For the FD MWPCs the efficiency has been determined for each of the six sensitive planes (two per chamber). At least two vertical and horizontal planes were demanded for track reconstruction and for the calculation of the intersection point with the remaining plane. Each plane has been divided in 20×20 subcells, and the efficiency of each cell has been calculated from the presence and absence of a hit in the reconstructed intersection. The average FD MWPC track efficiency for deuterons is 73%. The efficiencies of the scintillators and TOF criteria are larger than 99% [23]. The efficiency correction is done on an event-by-event basis.

## III. RESULTS FOR THE REACTION $pp \to d\pi^+\eta$

The missing mass distributions $mm(pp,d)$ and $mm(pp,d\pi^+)$ for the selected $d\pi^+$ pairs are presented in Fig. 3. In the $(pp,d\pi^+)$ missing mass distribution a clear peak is observed around m($\eta$)=547 MeV/c$^2$ with about 6200 events. The peak sits on top of a smooth background from multi-pion production $pp \to d\pi^+(n\pi)$ ($n \geq 2$). After selecting the mass range $(530 - 560)$ MeV/c$^2$ around the $\eta$ peak, the missing mass spectrum $mm(pp,d)$ exhibits a shoulder at 980 MeV/c$^2$ (Fig. 3a, dotted), where the peak from the $a_0^+(980)$ resonance is expected.

Table I presents the differential cross sections for $pp \to d\pi^+\eta$ for two regions of phase space where the acceptance of ANKE is essentially 100% for this reaction. Six variables in the lab. system have been chosen to describe these rectangular areas: the vertical ($\theta_y$) and horizontal ($\theta_x$) angles and momenta of the two detected particles, deuteron and $\pi^+$. These angles are defined as $\tan(\theta_y) = p_y/p_z$, $\tan(\theta_x) = p_x/p_z$.

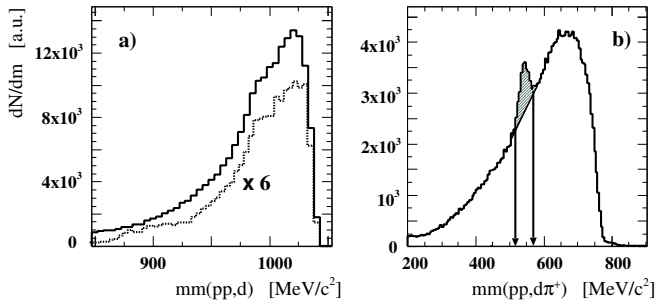


FIG. 3: Missing mass distributions (a) $mm(pp,d)$, (b) $mm(pp,d\pi^+)$ for the reaction $pp \to d\pi^+X$. The dotted histogram in $mm(pp,d)$ (scaled by factor 6) corresponds to the selected area around the $\eta$ peak ($530-560$ MeV/c$^2$) in $mm(pp,d\pi^+)$ (indicated by arrows).

| $\mathrm{d}^4\sigma/\mathrm{d}\Omega_d\mathrm{d}\Omega_{\pi^+}\mathrm{d}p_d\mathrm{d}p_{\pi^+}$ | variables, lab. system | | |
|---|---|---|---|
| $\mu$b/(sr GeV/c)$^2$ | $\theta_y$, deg. | $\theta_x$, deg. | $p$, GeV/c |
| $71 \pm 6_{\mathrm{stat}} \pm 20_{\mathrm{sys}}$ | deuteron variables | | |
| | $(-3^\circ,+3^\circ)$ | $(-3.5^\circ,+3.5^\circ)$ | $(1.4, 1.6)$ |
| | pion variables | | |
| | $(-4^\circ,+4^\circ)$ | $(-11^\circ,-3^\circ)$ | $(0.65, 0.95)$ |
| $30 \pm 4_{\mathrm{stat}} \pm 9_{\mathrm{sys}}$ | deuteron variables | | |
| | $(-3^\circ,+3^\circ)$ | $(-6^\circ,-2^\circ)$ | $(1.8, 2.7)$ |
| | pion variables | | |
| | $(-4^\circ,+4^\circ)$ | $(-11^\circ,-3^\circ)$ | $(0.65, 0.95)$ |

TABLE I: Differential production cross sections for the reaction $pp \to d\pi^+\eta$. In both regions of phase space $a_0^+$ and non-resonant $\pi^+\eta$ productions contribute. For the momentum range $p_d = (1.4-1.6)$ GeV/c the non-resonant $\pi^+\eta$ production should be dominant, because this momentum range corresponds to low masses of the $\pi^+\eta$ system, where the $a_0^+$ production is suppressed.

Unfortunately, due to the limited phase-space coverage of ANKE, a partial wave decomposition of the type performed in Ref. [20] is not possible in this case. Thus, in order to interpret the data in terms of $a_0^+$ and non–resonant $\pi^+\eta$ production, we need to employ a model. This investigation will be described in the next section.

## IV. INTERPRETATION OF THE RESULTS

The $d\pi^+\eta$ final state can be produced *via* the $a_0^+$ resonance, $pp \to da_0^+ \to d\pi^+\eta$ (resonant production), or through the direct reaction $pp \to d\pi^+\eta$ (non-resonant production). The production mechanism for the $a_0^+$ has been studied theoretically in Refs. [25, 26, 27, 28, 29]. According to Refs. [25, 26], the cross section for $a_0^+$ production at $T$=2.65 GeV is expected to be $\sim 1\mu$b while, for the non-resonant $\pi^+\eta$ production, different predictions exist, ranging from $(0.6-1.4)$ $\mu$b [30] and $(1.6-3.3)\mu$b [31] up to one order of magnitude more [26].

The differential cross sections from Table I contain contributions from both the resonant and the non-resonant reactions. We have performed a model-dependent analysis using the calculated momentum distributions of the produced deuterons (see Figs. 4a,b). The calculations are based on models describing the resonant process within the Quark-Gluon Strings Model (QGSM) (Fig. 5a) [32] and the non-resonant (Fig. 5b) production *via* $N^*$- and $\Delta$-resonance excitation [29, 31, 33]. The momentum distribution for the resonant reaction is narrower, because low $(\pi^+\eta)$ masses are suppressed for $a_0^+$ production. The momentum distributions within the ANKE acceptance are shown in Figs. 4c,d.

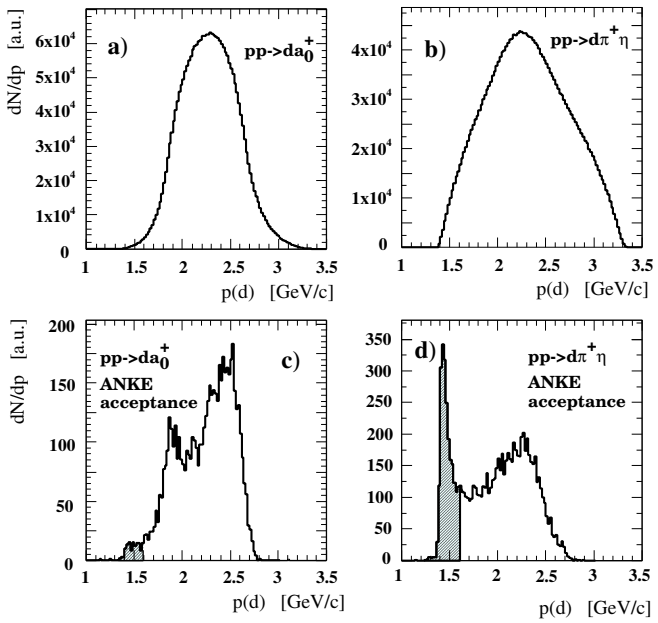


FIG. 4: Simulated acceptance for the deuteron momentum for the resonant (a,c) and the non-resonant (b,d) $\pi^+\eta$ production. Upper row: the initial model distributions [29, 31, 32, 33]; lower row: momentum distributions within the ANKE acceptance.

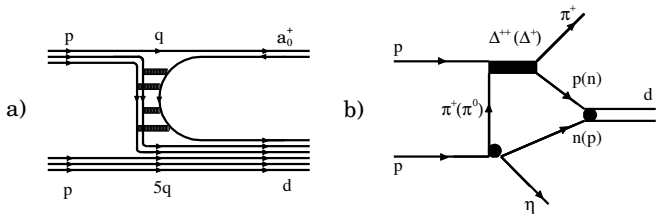


FIG. 5: Diagrams describing the resonant $\pi^+\eta$ production within the QGSM [32] (a) and the non-resonant *via* $N^*$ and $\Delta$ excitations [29, 31, 33] (b).

Within the models the non-resonant background has a negligible $\pi\eta$ $s$–wave contribution and thus does not interfere with the resonant amplitude. As a consequence, in the range $p_d = (1.4-1.6)$ GeV/c, the contribution of

the non-resonant process dominates whereas the resonant part is negligibly small (see shaded areas in Figs. 4c,d). Thus, the cross section of the non-resonant contribution in this momentum range can be defined by fitting the $\eta$ peak in $mm(pp, d\pi^+)$ (Fig. 6a) and extracting the number of $d\pi^+\eta$ events. The missing mass spectra have been described by the sum of a Gaussian distribution and a $4^{\text{th}}$ order polynomial.

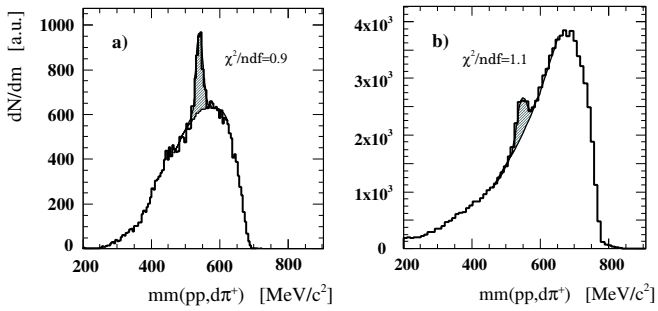


FIG. 6: Missing mass distribution $mm(pp, d\pi^+)$ for the momentum ranges $p_d = (1.4 - 1.6)$ GeV/c (a) and $p_d = (1.6 - 2.8)$ GeV/c (b).

In the momentum range $p_d = (1.6-2.8)$ GeV/c, where both the resonant and the non-resonant reactions contribute, it is possible to calculate the number of events from the non-resonant production taking into account the different acceptances. Then the number of $a_0^+$ events is the difference between the total number of events under the $\eta$ peak (Fig. 6b) and the calculated amount of non-resonant $\pi^+\eta$ events.

Including all corrections, total cross sections $\sigma_{\text{a}_0} = (1.1 \pm 0.3_{\text{stat}} \pm 0.7_{\text{sys}})$ $\mu$b for the $a_0^+$ production and $\sigma_{\text{n.r.}} = (3.5 \pm 0.3_{\text{stat}} \pm 1.0_{\text{sys}})$ $\mu$b for the non-resonant $\pi^+\eta$ production have been obtained. It is obvious, that these numbers could change if different assumptions were made on the partial wave decomposition of the (non–)resonant contributions. However, we here refrain from investigating further the uncertainty induced by the model assumptions.

Figure 7a presents the results of GEANT simulations of the ANKE acceptance for multipion background ($pp \to d\pi^+(n\pi)$ $(n \geq 2)$), and for resonant and non-resonant production of the $d\pi^+\eta$ final state. The number of initial events for each reaction is proportional to the known cross sections for multipion production [34] and the values of the total cross sections for the resonant and non-resonant $\pi^+\eta$ production given above. The shape of the simulated missing mass distribution $mm(pp, d)$ including all channels is in good agreement with the experimental data (Fig. 7b).

Data for the second $a_0^+$ decay channel, $a_0^+ \to K^+\bar{K^0}$, have been obtained at ANKE in the reaction $pp \to da_0^+ \to dK^+\bar{K^0}$, simultaneously with the $\pi^+\eta$ data. The measured total cross section is $\sigma(pp \to dK^+\bar{K^0}) = (38 \pm 2_{\text{stat}} \pm 14_{\text{sys}})$ nb and the contribution of the $(K^+\bar{K^0})_{L=0}$ channel is $\sim 83\%$ [20]. Assuming that $s$–wave $(K^+\bar{K^0})$ production proceeds fully *via* the $a_0^+(980)$ resonance,

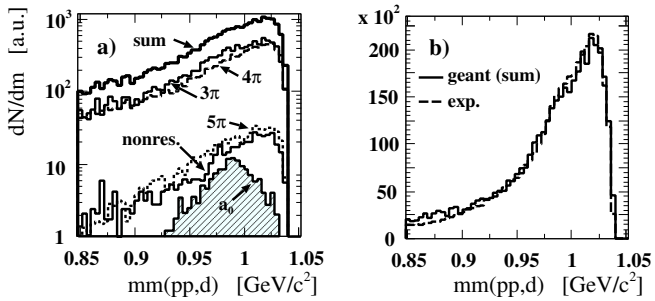


FIG. 7: a) GEANT simulations for multi-pion background ($pp \to d\pi^+(n\pi)$ $(n \geq 2)$), and for resonant and non-resonant production of the $d\pi^+\eta$ final state in the ANKE acceptance. b) comparison between the simulated missing mass distribution $mm(pp, d)$ and experimental data.

in accordance with the predictions of the models discussed above, the ratio of the total cross sections is $R = \sigma(a_0^+ \to (K^+\bar{K^0})_{L=0})/\sigma(a_0^+ \to \pi^+\eta) = 0.029 \pm 0.008_{\text{stat}} \pm 0.009_{\text{sys}}$.

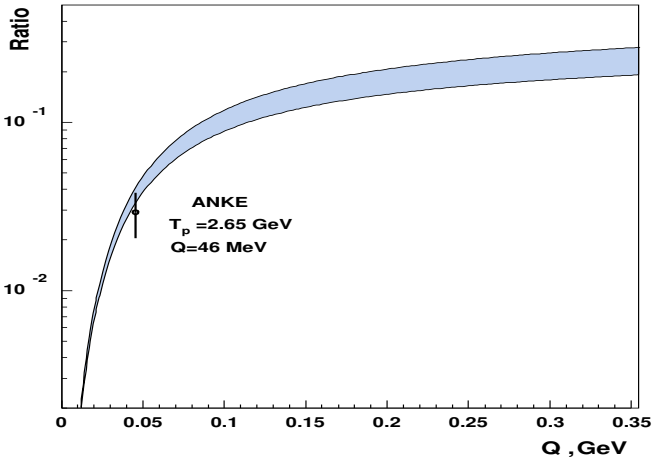


FIG. 8: Ratio of the total cross sections $\sigma(a_0^+ \to K^+\bar{K^0})/\sigma(a_0^+ \to \pi^+\eta)$ as function of $Q$. The error bar shows the statistical error only.

For measurements at an excess energy $Q >> \Gamma_{a_0} \sim (50 - 100)$ MeV, the ratio of the total cross sections $R = \sigma(a_0^+ \to K^+\bar{K^0})/\sigma(a_0^+ \to \pi^+\eta)$ should not depend upon $Q$. However, when $Q$ is of the order of $\Gamma_{a_0}$, the contribution from the $a_0^+ \to K^+\bar{K^0}$ decay channel decreases more strongly due to the proximity of the $K^+\bar{K^0}$ threshold and the consequently limited available phase space. The calculated ratio of the two cross sections as a function of $Q$ is presented in Fig. 8. The calculation is normalised to $R((K\bar{K})/(\pi\eta)) = 0.23 \pm 0.05$, which has been measured at Crystal Barrel in the reaction $p\bar{p} \to a_0\pi$ at $Q = 768$ MeV [35]. The parameters of the Flatté distribution [36] $m_0 = 999 \pm 2$ MeV/c$^2$, $g_{\pi\eta} = (324 \pm 15)$ MeV and $r = g^2_{KK}/g^2_{\pi\eta} = 1.03 \pm 0.14$ are also taken from Ref. [35]. The errors of the Flatté parameters define the range of possible $R$ values (shaded area in Fig. 8). Our result is in agreement with the calculated value.

## V. CONCLUSIONS

To summarize, data on the reaction $pp \to d\pi^+\eta$ at $T_p = 2.65$ GeV are presented. Differential cross sections for limited regions of phase space, corresponding to forward emission of the $d$ and $\pi^+$ in the laboratory system, have been extracted. Dynamical models for the reaction were employed to obtain the total cross sections for the resonant $\pi^+\eta$ production *via* the $a_0^+(980)$ and for the non-resonant $\pi^+\eta$ channel. For $a_0^+$ production the value for the total cross section $pp \to da_0^+ \to d\pi^+\eta$ is in agreement with theoretical predictions based on the value for the $pp \to d(K^+\bar{K^0})_{L=0}$ reaction recently measured at ANKE [20] and the branching ratio $BR(K\bar{K}/\pi\eta)$ from the literature.

Our results, together with those from ANKE on the decay channel $a_0^+ \to K^+\bar{K^0}$, are the first evidence for $a_0^+$ production in $pp$ collisions, obtained in a simultaneous exclusive measurement of both $a_0^+$ decay channels.

We are grateful to C. Wilkin for critical discussions and a careful reading of the manuscript. We would like to thank to W. Borgs, C. Schneider and the IKP technicians for the support during the beamtime. One of the authors (P.F.) acknowledges support by the COSY-FFE program (grant FFE-41520733). The work at ANKE has partially been supported by: BMBF (grants WTZ-RUS-686-99, 211-00, 691-01, GEO-001-99, POL-007-99, 015-01), DFG (436 RUS 113/444, 630, 733,787), DFG-RFBR 03-02-04013, 02-02-04001(436 RUS 113/652), Polish State Committee for Scientific Research (2 P03B 101 19), Russian Academy of Science (RFBR 06518, 02-02-16349), ISTC (1861, 1966).

[1] T. Kunihiro *et al.* [SCALAR Collaboration], arXiv:hep-ph/0308291.
[2] D. Morgan, Phys. Lett. B **51**, 71 (1974); K.L. Au, D. Morgan, and M.R. Pennington, Phys. Rev. D **35**, 1633 (1987); D. Morgan and M.R. Pennington, Phys. Lett. B **258**, 444 (1991); D. Morgan and M.R. Pennington, Phys. Rev. D **48**, 1185 (1993); A.V. Anisovich *et al.*, Eur. Phys. J. A **12**, 103 (2001); S. Narison, hep-ph/0012235.
[3] S. Eidelman *et al.* (Particle Data Group); Phys. Lett. B **592**, 1 (2004).
[4] J. Weinstein and N. Isgur, Phys. Rev. Lett. **48**, 659 (1982); Phys. Rev. D **27**, 588 (1983); Phys. Rev. D **41**, 2236 (1990); G. Janssen *et al.*, Phys. Rev. D **52**, 2690 (1995); J.A. Oller and E. Oset, Nucl. Phys. A **620**, 438 (1997) [Erratum-ibid. A **652**, 407 (1999)].
[5] N.N. Achasov, hep-ph/0201299; R.J. Jaffe, Phys. Rev. D **15**, 267 (1977); J. Vijande *et al.*, Proc. Int. Workshop MESON 2002, May 24–28, 2002, Cracow, Poland, World Scientific Publishing, ISBN 981-238-160-0, p.501, hep-ph/0206263.
[6] F.E. Close and N.A. Törnqvist, J. Phys. G **28**, R249 (2002).
[7] J.B. Gay *et al.*, Phys. Lett. B **63**, 220 (1976).
[8] A. Abele *et al.*, Phys. Lett. B **327**, 425 (1994); A. Abele *et al.*, Phys. Rev. D **57**, 3860 (1998); A. Bertin *et al.*, Phys. Lett. B **434**, 180 (1998).
[9] S. Teige *et al.*, Phys. Rev. D **59**, 012001 (1999).
[10] P. Achard *et al.*, Phys. Lett. B **526**, 269 (2002).
[11] N.N. Achasov *et al.*, Phys. Lett. B **485**, 349 (2000); Phys. Lett. B **479**, 53 (2000).
[12] A. Aloisio *et al.*, Phys. Lett. B **536**, 209 (2002); Phys. Lett. B **537**, 21 (2002).
[13] D. Barberis *et al.*, Phys. Lett. B **440**, 225 (1998); Phys. Lett. B **488**, 225 (2000).
[14] M.A. Abolins *et al.*, Phys. Rev. Lett. **25**, 469 (1970).
[15] R. Maier, Nucl. Instr. and Methods Phys. Res., Sect. A **390**, 1 (1997).
[16] M. Büscher, Acta Phys. Pol. B **35**, 1055 (2004).
[17] C. Hanhart, Phys. Rept. **397**, 155 (2004).
[18] N.N. Achasov *et al.*, Phys. Lett. B **88**, 367 (1979).
[19] S. Barsov *et al.*, Nucl. Instr. and Methods Phys. Res., Sect. A **462**, 364 (2001).
[20] V. Kleber *et al.*, Phys. Rev. Lett. **91**, 172304 (2003).
[21] R. Santo *et al.*, Nucl. Instr. and Methods Phys. Res., Sect. A **386**, 228 (1997); A. Khoukaz *et al.*, Eur. Phys. J. D **5**, 275 (1999).
[22] I. Zychor, Acta Phys. Pol. B **33**, 521 (2002).
[23] M. Büscher *et al.*, Nucl. Instr. and Methods Phys. Res., Sect. A **481**, 378 (2002).
[24] V. Komarov *et al.*, Phys. Lett. B **553**, 179 (2003).
[25] V.Y. Grishina *et al.*, Phys. Lett. B **521**, 217 (2001).
[26] H. Müller, Eur. Phys. J. A **11**, 113 (2001).
[27] E. Oset *et al.*, Eur. Phys. J. A **12**, 435 (2001).
[28] E.L. Bratkovskaya *et al.*, J. Phys. G **28**, 2423 (2002).
[29] L.A. Kondratyuk *et al.*, Phys. At. Nucl. **66**, 152 (2003) (Yad. Fiz., **66**, 155 (2003)).
[30] V.E. Tarasov and A.E. Kudryavtsev, private communication.
[31] V.Y. Grishina *et al.*, Annual Report 2000 of the IKP, FZ Jülich, p.30.
[32] V.Y. Grishina *et al.*, Eur. Phys. J. A **21**, 507 (2004).
[33] A.E. Kudryavtsev *et al.*, Phys. At. Nucl. **66**, 1946 (2003) (Yad. Fiz., vol. **66**, 1994 (2003)).
[34] A. Baldini, Landolt-Börnstein, New Ser. I, Vol. **12**, 97 (1988), reactions 71,72 and 73.
[35] A. Abele *et al.*, Phys. Rev. D **57**, 3860 (1998).
[36] S. Flatté, Phys. Lett. B **63**, 225 (1976).